



Published in final edited form as:

Neuroimage. 2022 April 15; 250: 118874. doi:10.1016/j.neuroimage.2022.118874.

Modulation of brain networks during MR-compatible transcranial direct current stimulation

Amber M. Leaver^{a,b,*}, Sara Gonzalez^b, Megha Vasavada^b, Antoni Kubicki^b, Mayank Jog^b, Danny J.J. Wang^c, Roger P. Woods^{b,d}, Randall Espinoza^d, Jacqueline Gollan^e, Todd Parrish^a, Katherine L. Narr^{b,d}

^aDepartment of Radiology, Northwestern University, Chicago, IL, 60611, United States

^bDepartment of Neurology, University of California Los Angeles, Los Angeles, CA, 90095, United States

^cLaboratory of FMRI Technology (LOFT), Stevens Neuroimaging and Informatics Institute, Keck School of Medicine, University of Southern California, Los Angeles CA 90033, United States

^dDepartment of Psychiatry and Biobehavioral Sciences, University of California Los Angeles, Los Angeles, CA, 90095, United States

^eDepartment of Psychiatry and Behavioral Sciences, Northwestern University, Chicago, IL, 60611, United States

Abstract

Transcranial direct current stimulation (tDCS) can influence performance on behavioral tasks and improve symptoms of brain conditions. Yet, it remains unclear precisely how tDCS affects brain function and connectivity. Here, we measured changes in functional connectivity (FC) metrics in blood-oxygenation-level-dependent (BOLD) fMRI data acquired during MR-compatible tDCS in a whole-brain analysis with corrections for false discovery rate. Volunteers ($n = 64$) received active tDCS, sham tDCS, and rest (no stimulation), using one of three previously established electrode tDCS montages targeting left dorsolateral prefrontal cortex (DLPFC, $n = 37$), lateral temporoparietal area (LTA, $n = 16$), or superior temporal cortex (STC, $n = 11$). In brain networks where simulated E field was highest in each montage, connectivity with remote nodes decreased during active tDCS. During active DLPFC-tDCS, connectivity decreased between a fronto-parietal network and subgenual ACC, while during LTA-tDCS connectivity decreased

This is an open access article under the CC BY-NC-ND license (<http://creativecommons.org/licenses/by-nc-nd/4.0/>)

*Corresponding author at: 737N Michigan Ave, Suite 1600, Chicago, IL 60611, United States. amber.leaver@northwestern.edu (A.M. Leaver).

CRedit Statement

All Authors: Writing- Review and editing. Amber Leaver: Conceptualization, Methodology, Investigation, Formal analysis, Visualization, Writing- Original draft preparation, Funding acquisition. Sara Gonzalez: Investigation, Project administration. Megha Vasavada, Antoni Kubicki, Roger Woods, Jacqueline Gollan: Investigation. Mayank Jog, Todd Parrish: Methodology. Danny Wang: Methodology, Funding acquisition. Randall Espinoza: Investigation, Funding acquisition. Katherine Narr: Conceptualization, Methodology, Investigation, Funding acquisition.

Declaration of Competing Interest

All authors declare no conflicts of interest.

Supplementary materials

Supplementary material associated with this article can be found, in the online version, at doi:10.1016/j.neuroimage.2022.118874.

between an auditory-somatomotor network and frontal operculum. Active DLPFC-tDCS was also associated with increased connectivity within an orbitofrontal network overlapping subgenual ACC. Irrespective of montage, FC metrics increased in sensorimotor and attention regions during both active and sham tDCS, which may reflect the cognitive-perceptual demands of tDCS. Taken together, these results indicate that tDCS may have both intended and unintended effects on ongoing brain activity, stressing the importance of including sham, stimulation-absent, and active comparators in basic science and clinical trials of tDCS.

Keywords

Transcranial direct current stimulation; fMRI; Functional connectivity

1. Introduction

Transcranial direct current stimulation (tDCS) is a form of noninvasive brain stimulation, where a constant, low-intensity electrical current is passed between two or more electrodes positioned on the head. The goal of tDCS research is to change brain activity to influence behavior, cognition, and the symptoms of a growing number of disorders (Stagg and Nitsche, 2011). As a potential treatment, tDCS is appealing because it is inexpensive, has the potential for supervised at-home use, and has little or no short or long-term side effects (Fregni et al., 2015; Matsumoto and Ugawa, 2017; Bikson et al., 2016). TDCS can thus potentially minimize patient burden associated with other forms of neurostimulation like transcranial magnetic stimulation (TMS) or electro-convulsive therapy (ECT). However, despite a growing number of tDCS studies, there is considerable skepticism regarding how (or whether) tDCS influences brain activity (Filmer et al., 2020). Evidence of the neurobiological mechanisms of tDCS is needed.

TDCS uses low-intensity electrical currents (1–2 mA) that influence neuronal membrane potential, which in turn influence spontaneous firing rates and neuronal excitability (Purpura and McMurtry, 1965; Creutzfeldt et al., 1962). The orientation and polarity of the electric (E) field also appear to matter: excitability increases when the E field is oriented parallel to pyramidal cells with dendrites near the anode (i.e., source of positive current), and decreases when the E field is oriented in the opposite direction (i.e., dendrites near the cathode) in animal models (Purpura and McMurtry, 1965; Creutzfeldt et al., 1962) and human studies (Nitsche and Paulus, 2000; Nitsche and Paulus, 2001). These elegant, straightforward findings have informed and explained electrode placement in human behavioral and clinical studies for decades, where tDCS anodes (or cathodes) are often positioned over regions the experimenter wishes to stimulate (or suppress). Indeed, this polarity-dependent model is supported by human studies, particularly those targeting motor cortex (Rawji et al., 2018; Mikkonen et al., 2018; Laakso et al., 2019; Stagg et al., 2009). However, the neurobiological effects of tDCS may be less straightforward in regions with variable/complex gyral anatomy, and the role of interneurons and downstream networks must also be considered (Stagg and Nitsche, 2011; Filmer et al., 2020; Liu et al., 2018).

This complexity is reflected in MRI studies measuring brain activity during concurrent tDCS. Again, studies targeting motor cortex with tDCS are perhaps most consistent, reporting disrupted motor cortex connectivity (Weinrich et al., 2017; Sehm et al., 2013) and increased thalamocortical connectivity (Polanía et al., 2012) during active stimulation, as well as increased motor cortex activity during active stimulation with concurrent motor tasks (Kwon and Jang, 2011). Studies targeting other brain regions have reported more disparate results, perhaps reflecting heterogeneity in tDCS targets and other aspects of experimental design (Li et al., 2022). Yet still other studies reported a lack of reliable change in brain activity measured with fMRI during active tDCS (Antal et al., 2011; Wörsching et al., 2017), or have demonstrated changes in BOLD-fMRI signal during active tDCS in *postmortem* brains (Antal et al., 2014), leading some to question the reliability of the technique (Jonker et al., 2021). These conflicting reports highlight the need for additional careful study of tDCS with fMRI and other neuroimaging techniques.

To empirically address how tDCS modulates activity in different brain networks, we measured the effects of tDCS on brain activity in humans during concurrent BOLD fMRI. Specifically, we hypothesized that resting-state functional connectivity would differ during active tDCS in brain regions and networks targeted by tDCS electrodes, when compared to sham tDCS, rest, and active comparators (i.e., active tDCS targeting other brain regions and networks). Three previously established electrode positions or “montages” were tested in this study (Fig. 1, (Loo et al., 2012; Fregni et al., 2006; Vanneste et al., 2013; Brunoni et al., 2017)) in parallel across three groups of volunteers (i.e., one montage per group) and under three experimental conditions: active tDCS, sham tDCS, and rest (no stimulation). Thus, our design included both sham and active comparators to mitigate any potential confounds related to the cognitive/perceptual experience of tDCS (e.g., somatosensations, anxiety, self-monitoring). The main analysis took an agnostic whole-brain (exploratory) approach, and measured interactions between tDCS montage and tDCS condition (active/sham/rest). We hypothesized that tDCS would influence brain regions where electrical current was high; therefore, additional analyses targeted brain regions and networks with high estimated E-field magnitude for each tDCS montage. Because tDCS is known to induce somatosensations during stimulation (e.g., tingling, itching), we hypothesized that the intensity of somatosensations during tDCS would influence brain function. Therefore, we also examined relationships between ratings of tDCS somatosensations and functional connectivity. Taken together, our study measured both the influence of electrical currents and cognitive/perceptual demands of tDCS on neurofunctional connectivity.

2. Materials methods

2.1. Subjects

Volunteers ($n = 64$) gave informed written consent for this study, with the approval of the Institutional Review Boards of UCLA and Northwestern University. Though not a focus of the current analyses, some volunteers had mild-to-moderate depression and/or chronic tinnitus. Breakdown of volunteer demographics and other study-related variables across the three tDCS montage groups can be found in Table 1 and Supplemental Methods.

2.2. Electrode preparation and positioning

Two $5 \times 7\text{cm}^2$ sponges wetted with saline (~ 7 mL per electrode) were each fitted to a $5 \times 5\text{mm}^2$ carbon rubber electrode. In addition to saline, a thin layer of conductive paste and gel were applied to the rubber electrode and sponge electrode cover, respectively, to prevent drying during the hour-long MRI scan.

Electrodes were positioned on the volunteer's head immediately before the MRI and secured with broad flexible bands made of rubber or vinyl. Electrodes were positioned with reference to the 10–10 EEG system in one of three montages (Fig. 1A), with long axis parallel to head circumference line (i.e., Fpz-Oz-Fpz). One group of volunteers received DLPFC-tDCS, with anode positioned over left dorsolateral prefrontal cortex (DLPFC, F3) and cathode positioned over right ventrolateral PFC (F8). In the LTA-tDCS group, the anode was placed over left temporoparietal cortex (LTA; halfway between C3 and T5), and cathode over right temporo-frontal cortex (halfway between F8 and T4). In the STC-tDCS group, the anode and cathode were placed over left (T3) and right (T4) temporal cortex, respectively. These montages were chosen based on their previous use in clinical studies (Jonker et al., 2021; Loo et al., 2012; Fregni et al., 2006; Vanneste et al., 2013). Electrode positions were checked visually before and after the scan, and during the scan by noting the position of the electrode on T1- and T2-weighted anatomical images.

2.3. tDCS stimulus delivery

Electrodes were connected to an MR-compatible stimulation device, including RF filters and resistors located on each wire. At Northwestern, electrodes were connected to a Soterix tES Device with HD-tDCS conversion box, which included an additional RF filter connector at the MR penetration panel. At UCLA, electrodes connected to a neuroConn tDCS device with wires passed through a “wave-guide” opening in the penetration panel, with RF filter box located near the opening. Setup followed manufacturer recommendations, and additional details can be found in Supplemental Methods.

TDCS amplitude was 2 mA, delivery was single-blind, and impedance was monitored before and throughout the entire scan to confirm manufacturer-recommended levels. For active tDCS, five minutes of 2 mA direct current was applied with 30-second linear ramps at the beginning and end of the five-minute stimulation period to minimize somatosensations. For sham tDCS, 2 mA stimulation began with a 30-second onset ramp immediately followed by 30-second offset ramp (and 4 min of no stimulation) to equate somatosensations between active and sham tDCS conditions. After this brief linear on-/off-ramp in the sham condition, no additional stimulation was applied. Electrodes remained in place for the duration of the scan, and were present for rest, active, and sham conditions.

BOLD-fMRI data were acquired during active tDCS, sham tDCS, and rest (no tDCS) for approximately 5 min per condition in each volunteer. Rest (no tDCS) condition was presented first, and order of active and sham scans was randomized and counter-balanced across volunteers. After active and sham tDCS, volunteers rated the intensity and discomfort associated with tDCS-related somatosensations on a 10-point Likert scale (0 = no sensation/discomfort; 10 = highest intensity/discomfort I can imagine). Active and sham tDCS scans

were separated by a 10–15 min “wash-out” period (i.e., during post-scan ratings and T1-weighted anatomical scan). Additional details regarding tDCS stimulus delivery may be found in the Supplemental Methods and Supplementary Figure 1.

2.4. MRI acquisition & preprocessing

MR images were acquired using 3T Prisma scanners at the UCLA Brain Mapping Center and Northwestern (NU) Center for Translational Imaging using identical sequences (Harms et al., 2018). Sequence parameters for BOLD-fMRI scans were as follows: 2 mm isotropic, 0.8 s repetition time (TR), 37 ms echo time (TE), 52° flip angle, 72 axial slices, 8 multiband factor. T1- and T2-weighted anatomical scans were also acquired: T1 multi-echo MPRAGE 0.8 mm isotropic, TR=2.5 s, TE=1.8, 3.6, 5.4, 7.2 ms combined, 1000 ms inversion time; 8° flip angle; T2 SPACE 0.8 mm isotropic, TR=3.2 s, TE=564 ms (effective TE of 559.7 ms), echo train length = 1166 ms.

BOLD-fMRI preprocessing was implemented using FSL, including motion correction and manual ICA-based denoising (Friston et al., 1996; Salimi-Khorshidi et al., 2014). Automated methods of ICA-based denoising (e.g., FSL’s ICA-FIX) do not include tDCS-fMRI data in their reference datasets used to train their classification algorithms; therefore, manual ICA-based denoising was chosen to ensure that preprocessed data were not contaminated by noise unique to tDCS that could be mis-labeled by the standard form of ICA-FIX. In brief, ICA was performed for each scan using FSL’s melodic, and ICs with spatial maps and temporal profiles judged consistent with neurobiological profiles (Griffanti et al., 2017) by A.M.L. were retained; other ICs were considered noise and filtered using FSL’s regfilt. Spatial image registration used FSL’s BBR tool, which includes nonlinear registration to a standard MNI template (Greve and Fischl, 2009). Finally, images were parcellated using the Schaeffer atlas (400 nodes (Schaefer et al., 2018)) in volume space as described below to improve signal-to-noise and reduce computational burden. All raw and preprocessed images passed visual inspection for quality.

2.5. Functional connectivity metrics

A number of FC metrics were calculated, including resting-state network (RSN) connectivity, local connectivity (regional homogeneity, ReHo (Jiang and Zuo, 2016)), and fractional amplitude of low frequency oscillations (fALFF; (Zou et al., 2008)). Each metric was calculated voxelwise in each condition block (active/sham/rest), then averaged within each node (Schaeffer 400-parcel atlas (Schaefer et al., 2018), Fig. 1) for statistical analysis as described further below.

RSNs were defined using the Yeo Atlas (17 networks liberal mask (Thomas Yeo et al., 2011), Fig. 1). FSL’s dual regression procedure (Nickerson et al., 2017) calculated the strength of temporal coherence between resting brain activity (i.e., BOLD-fMRI timecourse) of each voxel and the timecourse of each RSN. These connectivity values were averaged within each node to calculate node-to-network connectivity and averaged within each network to derive within-network connectivity.

The REST Toolkit (Song et al., 2011) calculated Regional Homogeneity (ReHo) and fractional Amplitude of Low Frequency Fluctuations (fALFF) in Matlab (R2019a,

Mathworks). ReHo reflects the neighborhood coherence the BOLD-fMRI timecourses within a given region, and is thought to reflect local connectivity. fALFF reflects the relative power of the neurobiologically relevant spectral content of the BOLD timecourse (0.01–0.1 Hz; (Song et al., 2011)). ReHo and fALFF were averaged within each node and network.

2.6. Statistical analyses

All statistical analyses were completed in R (<https://www.r-project.org>). Additional details, including all libraries used, can be found in Supplemental Methods.

Our primary analysis targeted a condition-by-montage interaction to capitalize on the inclusion of sham and active comparators in our study design, applied across the entire brain (i.e., all nodes and networks). Linear mixed models (Bates et al., 2015) were implemented, with condition (active, sham, rest), montage (DLPFC, LTA, STC) and age as fixed factors, and subject as a random factor. Main effects of tDCS condition were also measured in these same linear mixed models, to identify cases where functional connectivity differed across tDCS conditions in the same manner across all tDCS montages. *P*-values were estimated using the Kenward-Roger method (Bates et al., 2015; Kenward and Roger, 1997; Satterthwaite, 1946) and corrected for false discovery rate $q < 0.05$ across networks for global functional connectivity metrics, and across nodes for each regional functional connectivity metric. For nodes and networks meeting these criteria for significance, pairwise comparisons across tDCS conditions were reported within each montage.

A secondary analysis directly compared active and sham tDCS in E field “hot spots” identified for each montage using MRI data from a single template head. SimNIBS software (Windhoff et al., 2013; Thielscher et al., 2015) estimated E field distributions using finite element models for each tDCS montage on the template head using standard protocols. For each montage, we identified the five nodes with greatest E field magnitude (i.e., $|E|$ in V/m), as well as the RSNs overlapping those top 5 nodes. Linear mixed models were used as described above as an omnibus test, and planned *post-hoc* contrasts of active tDCS vs. sham tDCS were calculated separately for each montage. Again, *p* values were FDR-corrected $q < 0.05$ across global functional connectivity metrics, and across nodes for each regional functional connectivity metric. For nodes and networks meeting these criteria for significance, all pairwise comparisons of tDCS condition were reported within each montage.

Finally, we measured associations between FC metrics and behavioral ratings made immediately after active and sham tDCS of stimulation intensity and discomfort. Linear regression models identified brain regions and networks where functional connectivity metrics showed linear associations with these ratings. In one model, intensity rating was the factor of interest, while montage and age were nuisance factors. In the second model, discomfort rating was the factor of interest, and montage and age were nuisance factors. *P*-values were corrected for false discovery rate $q < 0.05$ across global FC metrics, and across nodes for each regional FC metric.

In these analyses, critical comparisons were primarily within-subjects (e.g., active vs. sham conditions), and so we anticipated that study site would have minimal (if any) effect on

our target outcomes. However, for nodes and networks meeting criteria for significance in the above analyses, we repeated each statistical test *post hoc* with site (i.e., UCLA/NU) as an additional nuisance factor. From these *post-hoc* tests, we examined statistics associated with each original significant effect to confirm that adding site as a nuisance factor did not influence target statistical outcomes. We also examined main effects of site (uncorrected) for each of these *post-hoc* tests for completeness.

3. Results

3.1. Main effects of tDCS condition in sensory and attention regions

No significant interactions between tDCS condition (active/sham/rest) and tDCS montage (DLPFC/LTA/STC) were noted in omnibus tests for any FC metric at the node or network level ($pFDR > 0.05$ for all). However, significant main effects of tDCS condition (active/sham/rest) were noted for fALFF and ReHo in sensory and motor cortical nodes, as well as anterior and posterior cingulate cortex and anterior insula (Fig. 2A). Within these nodes, pairwise comparisons between tDCS conditions calculated *post hoc* indicated that this main effect of tDCS condition was primarily driven by increased fALFF and/or ReHo during active and sham tDCS conditions compared to the stimulation-absent “rest” condition, particularly within sensory and motor cortical regions (Fig. 2B). This pattern was also apparent in pairwise comparisons between tDCS conditions done within each montage separately, where differences between sham and rest conditions appeared particularly robust (Fig. 2C, Supplemental Figure 2). Corresponding statistics are displayed in Supplemental Table 1 for representative nodes (including means, standard deviations, and confidence intervals for each condition).

3.2. Active tDCS modulates connectivity in networks with high E field

For each tDCS montage, a template head was used to identify the five nodes with greatest E field magnitude (i.e., $|E|$ in V/m) as well as the RSNs they overlapped (Fig. 3, Supplemental Table 2), and FC metrics during their respective active and sham tDCS conditions were compared (e.g., active DLPFC-tDCS vs. sham DLPFC-tDCS in high E field nodes and networks for DLPFC-tDCS).

Mean FC within the orbitofrontal network (RSN10) increased during active DLPFC-tDCS compared to sham and rest DLPFC-tDCS conditions ($pFDR < 0.05$; Fig. 4A&B). During LTA-tDCS and STC-tDCS, mean FC within this network did not differ across tDCS conditions (active/sham/rest; Fig. 4B).

In FC between nodes and networks, active tDCS was generally associated with reduced connectivity between high E field networks and single nodes outside these networks (Fig. 4C&D). During active DLPFC-tDCS, connectivity between a frontoparietal network and a node near subgenual ACC was significantly reduced compared to sham DLPFC-tDCS ($pFDR < 0.05$) and rest. Connectivity between this frontoparietal network and a node near the right superior parietal lobule also decreased during active DLPFC-tDCS compared to sham DLPFC-tDCS and rest. These node-network FC metrics did not differ across tDCS conditions during LTA-tDCS or STC-tDCS. During active LTA-tDCS, connectivity between

the auditory and ventral somatomotor network and nodes near the left frontal operculum decreased compared to sham LTA-tDCS ($pFDR < 0.05$) and rest. Connectivity between the default mode network and lateral occipital cortex (LOC) also decreased during active LTA-tDCS compared to sham LTA-tDCS ($pFDR < 0.05$) and rest. These two node-network FC metrics did not differ across tDCS conditions in DLPFC-tDCS or STC-tDCS. During STC-tDCS, no differences between active and sham tDCS were noted at our chosen threshold. However, at $p < 0.001$ reduced connectivity was noted during active STC-tDCS between a high E field network, “Frontoparietal 3,” and a remote node on the right temporal pole ($pFDR = 0.27$, Supplemental Figure 2). Corresponding statistics are displayed in Supplementary Table 3 (including means, standard deviations, and confidence intervals for each condition).

3.3. Connectivity in sensorimotor and attention regions associated with tDCS ratings

On average, ratings of the intensity and discomfort of tDCS-related somatosensations did not differ between active and sham tDCS (intensity: $F(1102) = 0.83$, $p = 0.36$; discomfort: $F(1114) = 1.14$, $p = 0.29$; Table 1). Discomfort ratings showed negative linear association with FC metric $fALFF$ bilaterally in nodes near posterior superior temporal sulcus (pSTS) and lateral occipital cortex (LOC; $pFDR < 0.05$, Fig. 5, Supplemental Table 4). Intensity ratings during sham and active tDCS showed negative linear association with connectivity between a secondary somatomotor network and two nodes: primary visual cortex and dorsal premotor cortex (dPMC) near the motor strip (Fig. 5, Supplemental Table 4).

3.4. Post-hoc assessment of study site

In nodes and networks meeting statistical criteria described in Sections 3.1-3.3, statistical analyses were repeated with study site as an additional nuisance factor. All target statistical outcomes remained identical or nearly identical to main tests, and no significant main effects of study site were noted (uncorrected $p > 0.05$, Supplementary Table 5).

4. Discussion

In this paper, we demonstrated that tDCS may modulate brain-network activity both via exogenous electrical stimulation as intended, as well as through the cognitive-perceptual experience of receiving tDCS. In brain networks where E field was highest in each montage, connectivity between target networks near electrodes and remote nodes decreased during active tDCS. For example, during active DLPFC-tDCS, connectivity decreased between a fronto-parietal network and subgenual ACC, while during LTA-tDCS connectivity decreased between an auditory-somatomotor network and frontal operculum. Active DLPFC-tDCS was also associated with increased connectivity within an orbitofrontal network overlapping subgenual ACC, suggesting that disrupted connectivity between target networks near electrodes and remote nodes during tDCS may result in disinhibition of these remote regions. Critically, we also demonstrated that brain-network activity changed during both active and sham tDCS in sensorimotor and attention regions irrespective of montage, which likely reflects the cognitive-perceptual demands of experiencing tDCS (e.g., tingling during stimulation, self-monitoring for adverse events). Indeed, participant ratings of tDCS intensity and discomfort also influenced connectivity in sensory and association regions.

Taken together, these results indicate that tDCS may have both intended and unintended effects on ongoing brain activity, stressing the importance of including sham, stimulation-absent, and active comparators in basic science and clinical trials of tDCS. Future studies will be critical in determining how the acute changes identified in the current study associate with long-term plasticity after tDCS.

4.1. Active tDCS decreases connectivity between high E field networks and remote nodes

A growing number of neuroimaging studies have measured regional- and network-level changes in brain function during and after tDCS (Filmer et al., 2020); however, a coherent understanding of the effects of tDCS on brain activity has yet to emerge. In our study, active tDCS was associated with decreased connectivity between high E-field networks and remote nodes during stimulation, which we interpret as disrupted network-level connectivity. This is in line with previous studies reporting disrupted motor cortex connectivity during tDCS targeting motor cortex (Weinrich et al., 2017; Sehm et al., 2013), as well as a number of tDCS and TMS studies reporting network-level changes after stimulation (Wang et al., 2014; Hermiller et al., 2019; Peña-Gómez et al., 2012; Park et al., 2013; Keeser et al., 2011). Whether decreased network-level connectivity during active tDCS associates with increased (or decreased) local activity near electrodes could be addressed by future studies combining resting-state FC and cerebral blood flow measurements (e.g., ASL-fMRI, PET-fMRI), or in animal models. Of note, active tDCS did not appear to influence connectivity metrics in high E field nodes, further suggesting the importance of network-level changes during stimulation (and perhaps reflecting the diffuse stimulation applied relative to the size of each node). Taken as a whole, the effects of noninvasive brain stimulation do not appear to be limited to the stimulation site, and network-level connectivity should be considered when designing neurostimulation research and exploratory clinical trials (Fischer et al., 2017; Kunze et al., 2016; Fox et al., 2012).

DLPFC-tDCS has been studied as a potential treatment for depression, where the intended target is left DLPFC, the target of the FDA-cleared rTMS therapy for depression (McClintock et al., 2018). In our study, active DLPFC-tDCS modulated network connectivity in prefrontal cortex, orbitofrontal cortex, and subgenual ACC, all previously implicated in the neurobiology of depression (Mayberg et al., 1999; Leaver et al., 2016a; Sheline et al., 2010). However, our E field models also showed that peak electrical current applied during DLPFC-tDCS occurred in right prefrontal and orbitofrontal regions, not left DLPFC as intended. This could explain outcomes in previous trials, which have not been successful (Loo et al., 2012; Brunoni et al., 2017; Brunoni et al., 2014). Nevertheless, our study showed that DLPFC-tDCS decreased connectivity between prefrontal regions (fronto-parietal network) and subgenual ACC, while also increasing connectivity within an orbitofrontal network (that included subgenual ACC). Similar patterns of connectivity between left DLPFC and subgenual ACC have been linked to successful antidepressant response to rTMS targeting left DLPFC (Fox et al., 2012; Weigand et al., 2018), and our data demonstrate that tDCS can modulate this circuit in similar ways, at least in principle. Future studies are needed that combine prospective E field modeling (or measurements (Jog et al., 2016; Jog et al., 2020)) with pre-treatment assessment of functional connectivity to improve targeting of specific brain networks. Assessing the long-term effects of repeated,

longer (e.g., 20-min) tDCS sessions on brain activity and the symptoms of depression and other neuropsychiatric disorders will also be informative.

LTA-tDCS and STC-tDCS were intended to target auditory cortex, and have been studied as a potential treatment for chronic tinnitus. Similar to the depression literature, randomized controlled trials of rTMS have had some success (Folmer et al., 2015), yet results of previous LTA- and STC-tDCS trials have been inconsistent (Fregni et al., 2006; Vanneste et al., 2013; Shekhawat et al., 2015), and few large-scale randomized sham-controlled trials have been conducted (Yuan et al., 2018; Wang et al., 2018). Inconsistent results in previous tDCS trials may be explained, at least in part, by imprecise targeting. Peak E field intensities in our models of LTA-tDCS did not occur in the intended target (Lockwood et al., 1998; Plewnia et al., 2007; Leaver et al., 2011) but rather in left somatomotor regions and middle temporal gyrus. In models of STC-tDCS, peak E field occurred in middle temporal gyrus and lateral inferior temporal gyrus, not the intended target of auditory cortex (i.e., superior temporal cortex). Nevertheless, our results demonstrated that active LTA-tDCS acutely decreases connectivity in brain regions relevant to tinnitus pathophysiology, including auditory cortex, frontal operculum overlapping anterior insula, and default mode network overlapping medial orbitofrontal cortex (Maudoux et al., 2012; Leaver et al., 2016b; Zimmerman et al., 2019). Our study may have been under-powered to assess the effects of active STC-tDCS, but trends toward decreased connectivity between a fronto-parietal network and right anterior temporal pole were noted. Taken together, our study demonstrates that tDCS appears to have the ability to perturb brain networks relevant to the neuropathophysiology of tinnitus and other disorders, but future studies are needed that leverage predictive models using E fields and other data to improve targeting and assess the long-term consequences of repeated tDCS sessions on brain activity and tinnitus symptoms.

4.2. Cognitive-perceptual demands of tDCS may have unintended effects on brain activity

When study volunteers and patients undergo noninvasive neurostimulation, they engage in a cognitive/perceptual experience or “task”. They are given instructions, for example to sit quietly and to alert staff to discomfort or adverse events, and they typically experience somatosensations as the electrical current passes through their skin. Our study demonstrated that these task demands may cause unintended changes in brain activity in somatosensory and attention-related brain regions, in addition to the intended changes in brain regions targeted with stimulation electrodes. For example, we show that both active and sham tDCS increased fALFF in sensorimotor and attention-related regions, suggesting increased temporal coherence in neurobiologically relevant frequencies in these regions. Indeed, connectivity showed a linear relationship with intensity and discomfort ratings in bilateral posterior STS and LOC, a site of multisensory integration (Beauchamp et al., 2008). This is critical information, as endogenous activity associated with the cognitive-perceptual demands of neurostimulation could attenuate or enhance the intended effects of the exogenous electrical (or other) energy applied by the neurostimulation technique, regardless of whether sensory or attention networks were the intended target. For example, a recent study demonstrated that transcranial alternating current stimulation (tACS) may entrain cortical neurons through transcutaneous (not transcranial) stimulation (Asamoah et

al., 2019). Taken together, these results speak to the critical need for sham, no-stim, and active comparators in tDCS trials and in basic science research of the neurobiological effects of tDCS and other neurostimulation technologies.

4.3. Limitations

There are a number of limitations that should be considered when interpreting and contextualizing the current study. Potential sources of variability or noise (e.g., depression or tinnitus status, variable sample size, site-specific parameters) may have increased Type II error making it more difficult to detect subtle changes in brain-network function in these analyses, and future studies designed *a priori* to address the questions raised here are needed. Yet, several steps were taken to mitigate these issues (e.g., strict multiple comparisons correction, examining effects of study site *post hoc*), and by combining these datasets we reached a sample size sufficient to detect effects of tDCS. In order to minimize the number of statistical tests, this study also used atlases to analyze cortical nodes and networks; studies using other atlases or voxel-wise analyses including non-cortical structures may yield different results. Similarly, we used E fields from a template head model to identify nodes and networks of peak electrical current for our studies; E field models tailored to each volunteer and/or study sample may yield more accurate representations (Laakso et al., 2019; Soleimani et al., 2021). E field is likely to be influenced by head size (which differs on average between men and women), cortical morphology, and other aspects of head tissue anatomy, all of which could be addressed in future studies designed to assess relationships between these factors and the effects of tDCS on brain function. Future studies are also needed to address neuroplastic changes occurring after full-session (i.e., 20–30 min) and multi-session tDCS, the potential impact of asymmetrical electrode placements on brain function when cortical organization differs due to handedness, as well as the impact of tDCS on other aspects of brain function beyond connectivity (e.g., task fMRI, baseline resting activity). Note too that ultra-brief stimulation similar in duration to standard sham stimulation in this study and many others may also have neurobiological consequences (Javadi et al., 2012; Fonteneau et al., 2019); studies designed to measure relationships between stimulus dose (e.g., amplitude, duration, waveform) and acute and long-term changes in brain function are needed.

5. Conclusions

Our data show that active tDCS can modulate functional connectivity in brain networks where the magnitude of applied electrical current is highest. Given the skepticism surrounding the therapeutic utility of tDCS (Filmer et al., 2020), these results support the promise of this simple, inexpensive technology. Our data also demonstrate that tDCS may have unintended consequences on brain function, highlighting potential pitfalls of this technique. E field models used in the current study also demonstrated that the common strategy of positioning the anode (cathode) over the brain region one wishes to stimulate (suppress) may not be accurate. Prospective E field modeling is clearly a necessity in tDCS and other forms of brain stimulation (Windhoff et al., 2013; Thielscher et al., 2015) and will be critical in informing accurate targeting in future studies. Both active and sham tDCS influenced brain function in sensorimotor and attention regions in our study, demonstrating

that the cognitive-perceptual experience of receiving both active and sham tDCS may have unintended effects on brain function (though effects of brief E field applied during sham tDCS should also be considered). Blinding adequacy is an ongoing conversation in the field (Fonteneau et al., 2019; Wallace et al., 2016; O'Connell et al., 2012), and given that volunteers must always be informed of potential adverse events (even if rare) it is likely that volunteers will continue monitoring for skin sensations even if blocked by local anesthetic. Thus, our data highlight an important role for both active- and sham-comparators in noninvasive neurostimulation studies, and stress the importance of understanding how these unintended effects of tDCS on sensorimotor and attention regions may interact with the intended effects of electrical stimulation in target brain regions and networks in future research. Clearly, there is still much to understand regarding the effects of tDCS and other forms of neurostimulation on brain function. In these efforts, prospective planning of E field distribution and network connectivity will be key, both in improving targeting of specific brain networks and in understanding the role of inter-individual neuroanatomical variability on resulting E fields and neuroplastic outcomes to guide the successful translation of tDCS to different clinical settings.

Supplementary Material

Refer to Web version on PubMed Central for supplementary material.

Acknowledgements

This work was supported by NIH R21 DC015880 (A.M.L.), NIH R61 MH110526 (K.L.N., R.E., D.J.J.W.), a research grant from the American Tinnitus Association (A.M.L.), and a Young Investigator Award from the Brian and Behavior Research Foundation (A.M.L.).

Data and code availability statement

Data are available by request to the Authors pending a formal institutional data sharing agreement.

References

- Antal A, et al. , 2014. Imaging artifacts induced by electrical stimulation during conventional fMRI of the brain. *NeuroImage* 85 (03). doi:10.1016/j.neuroimage.2012.10.026.
- Antal A, Polania R, Schmidt-Samoa C, Dechent P, Paulus W, 2011. Transcranial direct current stimulation over the primary motor cortex during fMRI. *NeuroImage* 55 (2), 590–596. doi:10.1016/j.neuroimage.2010.11.085. [PubMed: 21211569]
- Asamoah B, Khatoun A, Mc Laughlin M, 2019. tACS motor system effects can be caused by transcutaneous stimulation of peripheral nerves. *Nat. Commun* 10 (1). doi:10.1038/s41467-018-08183-w, Art. no. 1. [PubMed: 30602773]
- Bates Douglas, Mächler Martin, Bolker Ben, Walker Steve, 2015. Fitting linear mixed-effects models using lme4. *J. Stat. Softw* 67 (1). doi:10.18637/jss.v067.i01.
- Beauchamp MS, Yasar NE, Frye RE, Ro T, 2008. Touch, sound and vision in human superior temporal sulcus. *NeuroImage* 41 (3), 1011–1020. doi:10.1016/j.neuroimage.2008.03.015. [PubMed: 18440831]
- Bikson M, et al. , 2016. Safety of transcranial direct current stimulation: evidence based update 2016. *Brain Stimulat.* 9 (5), 641–661. doi:10.1016/j.brs.2016.06.004.

- Brunoni AR, et al. , 2017. Trial of electrical direct-current therapy versus escitalopram for depression. *N. Engl. J. Med* 376 (26), 2523–2533. doi:10.1056/NEJMoa1612999. [PubMed: 28657871]
- Brunoni AR, Schestatsky P, Lotufo PA, Benseñor IM, Fregni F, 2014. Comparison of blinding effectiveness between sham tDCS and placebo sertraline in a 6-week major depression randomized clinical trial. *Clin. Neurophysiol* 125 (2), 298–305. doi:10.1016/j.clinph.2013.07.020. [PubMed: 23994192]
- Creutzfeldt OD, Fromm GH, Kapp H, 1962. Influence of transcortical d-c currents on cortical neuronal activity. *Exp. Neurol* 5, 436–452. doi:10.1016/0014-4886(62)90056-0. [PubMed: 13882165]
- Filmer HL, Mattingley JB, Dux PE, 2020. Modulating brain activity and behaviour with tDCS: rumours of its death have been greatly exaggerated. *Cortex* 123, 141–151. doi:10.1016/j.cortex.2019.10.006. [PubMed: 31783223]
- Fischer DB, et al. , 2017. Multifocal tDCS targeting the resting state motor network increases cortical excitability beyond traditional tDCS targeting unilateral motor cortex. *NeuroImage* 157, 34–44. doi:10.1016/j.neuroimage.2017.05.060. [PubMed: 28572060]
- Folmer RL, Theodoroff SM, Casiana L, Shi Y, Griest S, Vachhani J, 2015. Repetitive transcranial magnetic stimulation treatment for chronic tinnitus: a randomized clinical trial. *JAMA Otolaryngol.–Head Neck Surg* 141 (8), 716–722. doi:10.1001/jamaoto.2015.1219. [PubMed: 26181507]
- Fonteneau C, et al. , 2019. Sham tDCS: a hidden source of variability? Reflections for further blinded, controlled trials. *Brain Stimulat.* 12 (3), 668–673. doi:10.1016/j.brs.2018.12.977.
- Fox MD, Buckner RL, White MP, Greicius MD, Pascual-Leone A, 2012. Efficacy of TMS targets for depression is related to intrinsic functional connectivity with the subgenual cingulate. *Biol. Psychiatry* 72 (7), 595–603. doi:10.1016/j.biopsych.2012.04.028. [PubMed: 22658708]
- Fregni F, et al. , 2006. Transient tinnitus suppression induced by repetitive transcranial magnetic stimulation and transcranial direct current stimulation. *Eur. J. Neurol* 13 (9), 996–1001. doi:10.1111/j.1468-1331.2006.01414.x. [PubMed: 16930367]
- Fregni F, et al. , 2015. Regulatory considerations for the clinical and research use of transcranial direct current stimulation (tDCS): review and recommendations from an expert panel. *Clin. Res. Regul. Aff* 32 (1), 22–35. doi:10.3109/10601333.2015.980944. [PubMed: 25983531]
- Friston KJ, Williams S, Howard R, Frackowiak RSJ, Turner R, 1996. Movement-related effects in fMRI time-series. *Magn. Reson. Med* 35 (3), 346–355. doi:10.1002/mrm.1910350312. [PubMed: 8699946]
- Greve DN, Fischl B, 2009. Accurate and robust brain image alignment using boundary-based registration. *NeuroImage* 48 (1), 63–72. doi:10.1016/j.neuroimage.2009.06.060. [PubMed: 19573611]
- Griffanti L, et al. , 2017. Hand classification of fMRI ICA noise components. *NeuroImage* 154, 188–205. doi:10.1016/j.neuroimage.2016.12.036. [PubMed: 27989777]
- Harms MP, et al. , 2018. Extending the human connectome project across ages: imaging protocols for the lifespan development and aging projects. *NeuroImage* 183, 972–984. doi:10.1016/j.neuroimage.2018.09.060. [PubMed: 30261308]
- Hermiller MS, VanHaerents S, Raj T, Voss JL, 2019. Frequency-specific noninvasive modulation of memory retrieval and its relationship with hippocampal network connectivity. *Hippocampus* 29 (7), 595–609. doi:10.1002/hipo.23054. [PubMed: 30447076]
- Javadi AH, Cheng P, Walsh V, 2012. Short duration transcranial direct current stimulation (tDCS) modulates verbal memory. *Brain Stimulat.* 5 (4), 468–474. doi:10.1016/j.brs.2011.08.003.
- Jiang L, Zuo X-N, 2016. Regional homogeneity: a multimodal, multiscale neuroimaging marker of the human connectome. *Neuroscientist* 22 (5), 486–505. doi:10.1177/1073858415595004. [PubMed: 26170004]
- Jog MV, et al. , 2016. In-vivo imaging of magnetic fields induced by transcranial direct current stimulation (tDCS) in human brain using MRI. *Sci. Rep* 6 (1). doi:10.1038/srep34385, Art. no. 1. [PubMed: 28442746]
- Jog M, et al. , 2020. Concurrent imaging of markers of current flow and neurophysiological changes during tDCS. *Front. Neurosci* 14, 374. doi:10.3389/fnins.2020.00374. [PubMed: 32372913]

- Jonker ZD, Gaiser C, Tulen JHM, Ribbers GM, Frens MA, Selles RW, 2021. No effect of anodal tDCS on motor cortical excitability and no evidence for responders in a large double-blind placebo-controlled trial. *Brain Stimulat.* 14 (1), 100–109. doi:10.1016/j.brs.2020.11.005.
- Keeser D, et al. , 2011. Prefrontal transcranial direct current stimulation changes connectivity of resting-state networks during fMRI. *J. Neurosci* 31 (43), 15284–15293. doi:10.1523/JNEUROSCI.0542-11.2011. [PubMed: 22031874]
- Kenward MG, Roger JH, 1997. Small sample inference for fixed effects from restricted maximum likelihood. *Biometrics* 53 (3), 983–997. doi:10.2307/2533558. [PubMed: 9333350]
- Kunze T, Hunold A, Haueisen J, Jirsa V, Spiegler A, 2016. Transcranial direct current stimulation changes resting state functional connectivity: a large-scale brain network modeling study. *NeuroImage* 140, 174–187. doi:10.1016/j.neuroimage.2016.02.015. [PubMed: 26883068]
- Kwon YH, Jang SH, 2011. The enhanced cortical activation induced by transcranial direct current stimulation during hand movements. *Neurosci. Lett* 492 (2), 105–108. doi:10.1016/j.neulet.2011.01.066. [PubMed: 21291959]
- Laakso I, Mikkonen M, Koyama S, Hirata A, Tanaka S, Dec. 2019. Can electric fields explain inter-individual variability in transcranial direct current stimulation of the motor cortex? *Sci. Rep* 9 (1), 626. doi:10.1038/s41598-018-37226-x. [PubMed: 30679770]
- Leaver AM, et al. , 2016a. Plasticity of striato-frontal connectivity in major depressive disorder. *Cereb. Cortex* 26 (11), 4337–4346. doi:10.1093/cercor/bhv207, 17. [PubMed: 26400916]
- Leaver AM, Renier L, Chevillet MA, Morgan S, Kim HJ, Rauschecker JP, 2011. Dysregulation of limbic and auditory networks in tinnitus. *Neuron* 69 (1), 33–43. doi:10.1016/j.neuron.2010.12.002. [PubMed: 21220097]
- Leaver AM, Turesky TK, Seydell-Greenwald A, Morgan S, Kim HJ, Rauschecker JP, 2016b. Intrinsic network activity in tinnitus investigated with functional MRI. *Hum. Brain Mapp* 37 (8), 2717–2735. doi:10.1002/hbm.23204. [PubMed: 27091485]
- Li LM, et al. , 2022. Brain state and polarity dependent modulation of brain networks by transcranial direct current stimulation. *Hum. Brain Mapp* 0 (0). doi:10.1002/hbm.24420.
- Liu A, et al. , 2018. Immediate neurophysiological effects of transcranial electrical stimulation. *Nat. Commun* 9 (1). doi:10.1038/s41467-018-07233-7, Art. No. 1. [PubMed: 29317637]
- Lockwood AH, Salvi RJ, Coad ML, Towsley ML, Wack DS, Murphy BW, 1998. The functional neuroanatomy of tinnitus: evidence for limbic system links and neural plasticity. *Neurology* 50 (1), 114–120. doi:10.1212/wnl.50.1.114. [PubMed: 9443467]
- Loo CK, Alonzo A, Martin D, Mitchell PB, Galvez V, Sachdev P, 2012. Transcranial direct current stimulation for depression: 3-week, randomized, sham-controlled trial. *Br. J. Psychiatry* 200 (1), 52–59. doi:10.1192/bjp.bp.111.097634. [PubMed: 22215866]
- Matsumoto H, Ugawa Y, 2017. Adverse events of tDCS and tACS: a review. *Clin. Neurophysiol. Pract* 2, 19–25. doi:10.1016/j.cnp.2016.12.003. [PubMed: 30214966]
- Maudoux A, et al. , 2012. Connectivity graph analysis of the auditory resting state network in tinnitus. *Brain Res.* 1485, 10–21. doi:10.1016/j.brainres.2012.05.006. [PubMed: 22579727]
- Mayberg HS, et al. , 1999. Reciprocal limbic-cortical function and negative mood: converging PET findings in depression and normal sadness. *Am J Psychiatry* 156 (5), 675–682. [PubMed: 10327898]
- McClintock SM, et al. , 2018. Consensus recommendations for the clinical application of repetitive transcranial magnetic stimulation (rTMS) in the treatment of depression. *J. Clin. Psychiatry* 79 (1). doi:10.4088/JCP.16cs10905.
- Mikkonen M, Laakso I, Sumiya M, Koyama S, Hirata A, Tanaka S, 2018. TMS motor thresholds correlate with TDCS electric field strengths in hand motor area. *Front. Neurosci* 12. doi:10.3389/fnins.2018.00426.
- Nickerson LD, Smith SM, Öngür D, Beckmann CF, 2017. Using dual regression to investigate network shape and amplitude in functional connectivity analyses. *Front. Neurosci* 11. doi:10.3389/fnins.2017.00115.
- Nitsche MA, Paulus W, 2000. Excitability changes induced in the human motor cortex by weak transcranial direct current stimulation. *J. Physiol* 527 (Pt 3), 633–639. doi:10.1111/j.1469-7793.2000.t01-1-00633.x. [PubMed: 10990547]

- Nitsche MA, Paulus W, 2001. Sustained excitability elevations induced by transcranial DC motor cortex stimulation in humans. *Neurology* 57 (10), 1899–1901. doi:10.1212/wnl.57.10.1899. [PubMed: 11723286]
- O’Connell NE, et al. , 2012. Rethinking clinical trials of transcranial direct current stimulation: participant and assessor blinding is inadequate at intensities of 2 mA. *PLoS ONE* 7 (10), e47514. doi:10.1371/journal.pone.0047514. [PubMed: 23082174]
- Park C, Chang WH, Park J-Y, Shin Y-I, Kim ST, Kim Y-H, 2013. Transcranial direct current stimulation increases resting state interhemispheric connectivity. *Neurosci. Lett* 539, 7–10. doi:10.1016/j.neulet.2013.01.047. [PubMed: 23416318]
- Peña-Gómez C, et al. , 2012. Modulation of large-scale brain networks by transcranial direct current stimulation evidenced by resting-state functional MRI. *Brain Stimulat* 5 (3), 252–263. doi:10.1016/j.brs.2011.08.006.
- Plewnia C, et al. , 2007. Dose-dependent attenuation of auditory phantom perception (tinnitus) by PET-guided repetitive transcranial magnetic stimulation. *Hum. Brain Mapp* 28 (3), 238–246. doi:10.1002/hbm.20270. [PubMed: 16773635]
- Polanía R, Paulus W, Nitsche MA, 2012. Modulating cortico-striatal and thalamocortical functional connectivity with transcranial direct current stimulation. *Hum. Brain Mapp* 33 (10), 2499–2508. doi:10.1002/hbm.21380. [PubMed: 21922602]
- Purpura DP, McMurtry JG, 1965. Intracellular activities and evoked potential changes during polarization of motor cortex. *J. Neurophysiol* 28 (1), 166–185. doi:10.1152/jn.1965.28.1.166. [PubMed: 14244793]
- Rawji V, et al. , 2018. tDCS changes in motor excitability are specific to orientation of current flow. *Brain Stimulat* 11 (2), 289–298. doi:10.1016/j.brs.2017.11.001.
- Salimi-Khorshidi G, Douaud G, Beckmann CF, Glasser MF, Griffanti L, Smith SM, 2014. Automatic denoising of functional MRI data: combining independent component analysis and hierarchical fusion of classifiers. *NeuroImage* 90, 449–468. doi:10.1016/j.neuroimage.2013.11.046. [PubMed: 24389422]
- Satterthwaite FE, 1946. An approximate distribution of estimates of variance components. *Biom. Bull* 2 (6), 110–114. doi:10.2307/3002019.
- Schaefer A, et al. , 2018. Local-global parcellation of the human cerebral cortex from intrinsic functional connectivity MRI. *Cereb. Cortex N. Y. N* 1991 28 (9), 3095–3114. doi:10.1093/cercor/bhx179, 01.
- Sehm B, Kipping J, Schäfer A, Villringer A, Ragert P, 2013. A comparison between uni- and bilateral tDCS effects on functional connectivity of the human motor cortex. *Front. Hum. Neurosci* 7. doi:10.3389/fnhum.2013.00183.
- Shekhawat GS, Stinear CM, Searchfield GD, 2015. Modulation of perception or emotion? A scoping review of tinnitus neuromodulation using transcranial direct current stimulation. *Neurorehabil. Neural Repair* 29 (9), 837–846. doi:10.1177/1545968314567152. [PubMed: 25670225]
- Sheline YI, Price JL, Yan Z, Mintun MA, 2010. Resting-state functional MRI in depression unmasks increased connectivity between networks via the dorsal nexus. *Proc. Natl. Acad. Sci* 107 (24), 11020–11025. doi:10.1073/pnas.1000446107. [PubMed: 20534464]
- Soleimani G, et al. , 2021. Group and individual level variations between symmetric and asymmetric DLPFC montages for tDCS over large scale brain network nodes. *Sci. Rep* 11 (1), 1271. doi:10.1038/s41598-020-80279-0. [PubMed: 33446802]
- Song XW, et al. , 2011. REST: a Toolkit for resting-state functional magnetic resonance imaging data processing. *PLoS ONE* 6 (9). doi:10.1371/journal.pone.0025031.
- Stagg CJ, et al. , 2009. Polarity-sensitive modulation of cortical neurotransmitters by transcranial stimulation. *J. Neurosci* 29 (16), 5202–5206. doi:10.1523/JNEUROSCI.4432-08.2009. [PubMed: 19386916]
- Stagg CJ, Nitsche MA, 2011. Physiological basis of transcranial direct current stimulation. *Neurosci. Rev. J. Bringing Neurobiol. Neurol. Psychiatry* 17 (1), 37–53. doi:10.1177/1073858410386614.
- Thielscher A, Antunes A, Saturnino GB, 2015. Field modeling for transcranial magnetic stimulation: a useful tool to understand the physiological effects of TMS? In: 2015 37th Annual International

- Conference of the IEEE Engineering in Medicine and Biology Society (EMBC), pp. 222–225. doi:10.1109/EMBC.2015.7318340.
- Thomas Yeo BT, et al. , 2011. The organization of the human cerebral cortex estimated by intrinsic functional connectivity. *J. Neurophysiol* 106 (3), 1125–1165. doi:10.1152/jn.00338.2011. [PubMed: 21653723]
- Vanneste S, Fregni F, De Ridder D, 2013. Head-to-head comparison of transcranial random noise stimulation, transcranial AC stimulation, and transcranial DC stimulation for tinnitus. *Front. Psychiatry* 4. doi:10.3389/fpsyt.2013.00158.
- Wallace D, Cooper NR, Paulmann S, Fitzgerald PB, Russo R, 2016. Perceived comfort and blinding efficacy in randomised sham-controlled transcranial direct current stimulation (tDCS) trials at 2mA in young and older healthy adults. *PLoS ONE* 11 (2), e0149703. doi:10.1371/journal.pone.0149703. [PubMed: 26900961]
- Wang JX, et al. , 2014. Targeted enhancement of cortical-hippocampal brain networks and associative memory. *Science* 345 (6200), 1054–1057. doi:10.1126/science.1252900. [PubMed: 25170153]
- Wang T-C, et al. , 2018. Effect of transcranial direct current stimulation in patients with tinnitus: a meta-analysis and systematic review. *Ann. Otol. Rhinol. Laryngol* 127 (2), 79–88. doi:10.1177/0003489417744317. [PubMed: 29192507]
- Weigand A, et al. , 2018. Prospective validation that subgenual connectivity predicts antidepressant efficacy of transcranial magnetic stimulation sites. *Biol. Psychiatry* 84 (1), 28–37. doi:10.1016/j.biopsych.2017.10.028, 01. [PubMed: 29274805]
- Weinrich CA, Brittain J-S, Nowak M, Salimi-Khorshidi R, Brown P, Stagg CJ, 2017. Modulation of long-range connectivity patterns via frequency-specific stimulation of human cortex. *Curr. Biol. CB* 27 (19), 3061–3068. doi:10.1016/j.cub.2017.08.075, e3. [PubMed: 28966091]
- Windhoff M, Opitz A, Thielscher A, 2013. Electric field calculations in brain stimulation based on finite elements: an optimized processing pipeline for the generation and usage of accurate individual head models. *Hum. Brain Mapp* 34 (4), 923–935. doi:10.1002/hbm.21479. [PubMed: 22109746]
- Wörsching J, et al. , 2017. Test-retest reliability of prefrontal transcranial Direct Current Stimulation (tDCS) effects on functional MRI connectivity in healthy subjects. *NeuroImage* 155, 187–201. doi:10.1016/j.neuroimage.2017.04.052. [PubMed: 28450138]
- Yuan T, Yadollahpour A, Salgado-Ramírez J, Robles-Camarillo D, Ortega-Palacios R, 2018. Transcranial direct current stimulation for the treatment of tinnitus: a review of clinical trials and mechanisms of action. *BMC Neurosci.* 19 (1), 66. doi:10.1186/s12868-018-0467-3. [PubMed: 30359234]
- Zimmerman BJ, Abraham I, Schmidt SA, Baryshnikov Y, Husain FT, 2019. Dissociating tinnitus patients from healthy controls using resting-state cyclicity analysis and clustering. *Netw. Neurosci. Camb. Mass* 3 (1), 67–89. doi:10.1162/netn_a_00053.
- Zou Q-H, et al. , 2008. An improved approach to detection of amplitude of low-frequency fluctuation (ALFF) for resting-state fMRI: fractional ALFF. *J. Neurosci. Methods* 172 (1), 137–141. doi:10.1016/j.jneumeth.2008.04.012. [PubMed: 18501969]

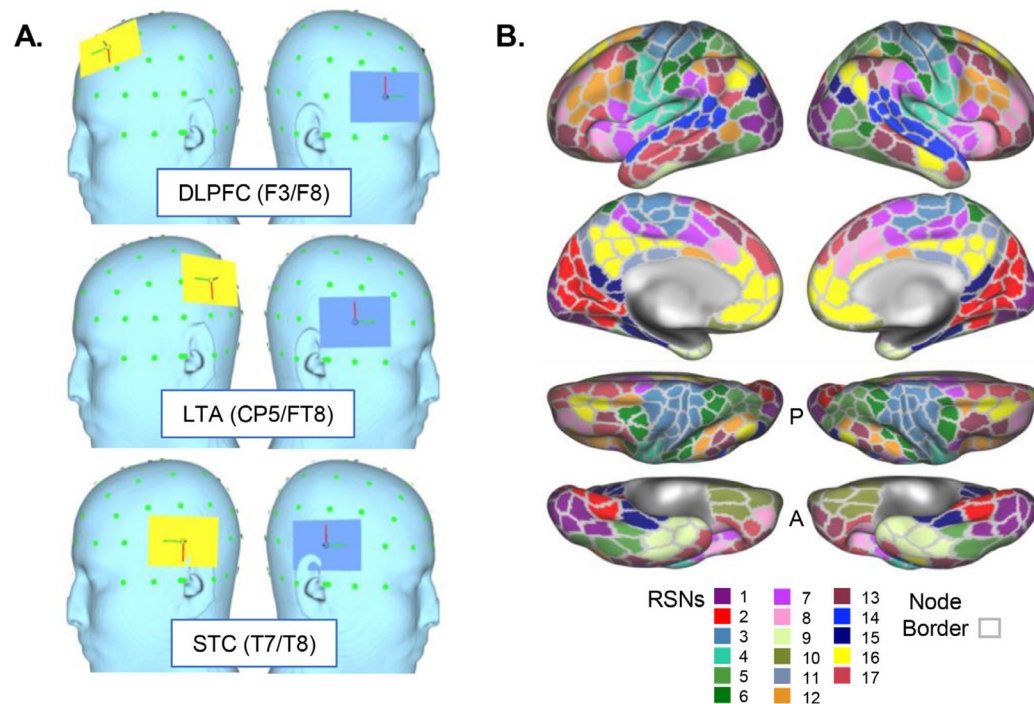


Fig. 1.

Electrode positions and resting state networks (RSNs) used in the current study. A. Electrode positions (“montages”) are displayed on the reconstructed surface of a template head, including DLPFC (dorsolateral prefrontal cortex), LTA (lateral temporoparietal area), and STC (superior temporal cortex). Anode is displayed in yellow and cathode in blue. 10–10 EEG positions are also displayed for each montage; green dots mark the visible 10–10 EEG grid. B. Resting state network (RSN) atlas is displayed, as derived from the 17-network template in Yeo et al. 2011. Each network is given a color as indicated by the key at bottom and is displayed on reconstructed cortical surfaces (from top to bottom: lateral, medial, dorsal, ventral). Gray outlines also indicate nodes used in the current analyses, derived from the 400-parcel template from Schaeffer et al. 2018.

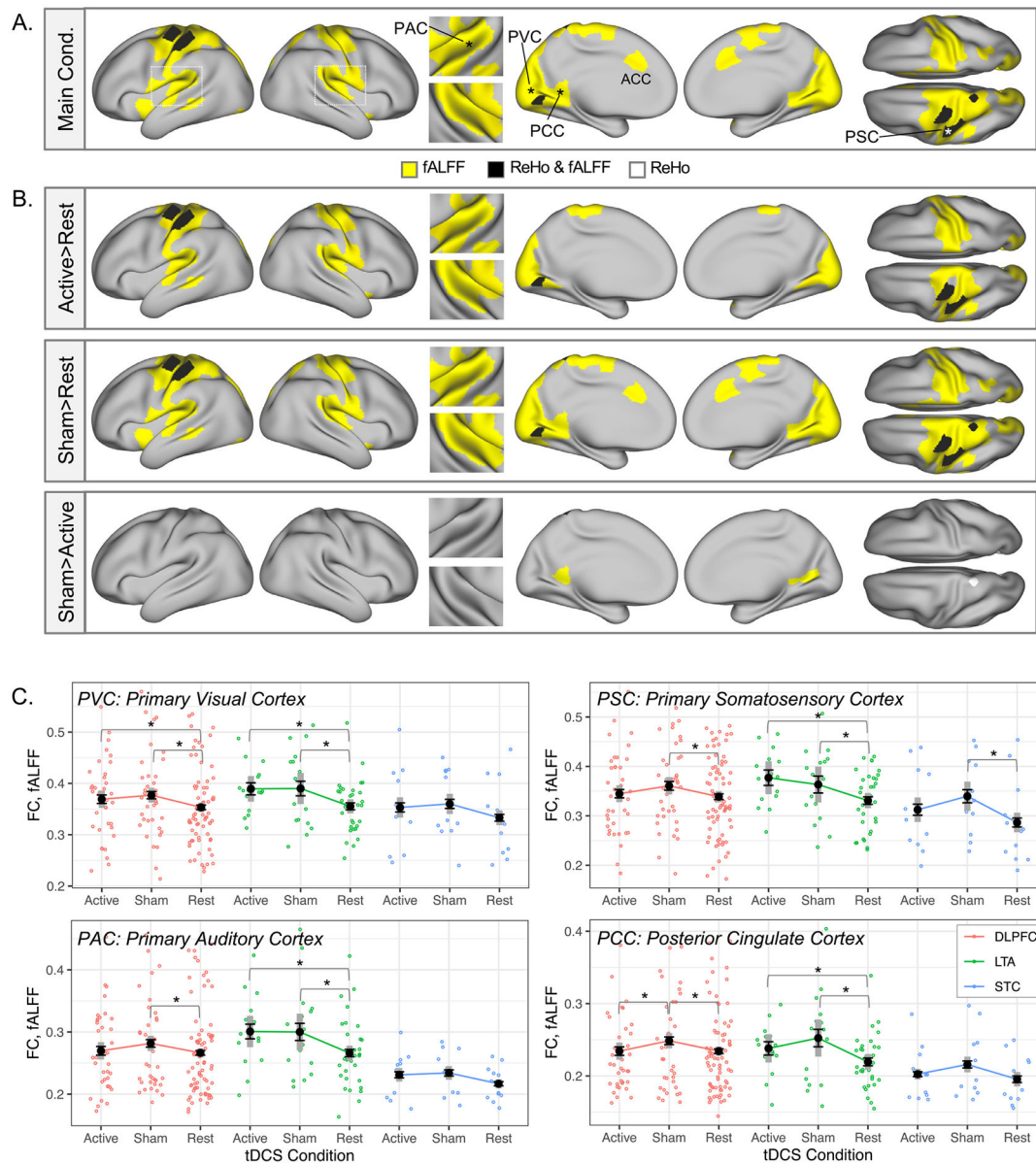


Fig. 2. Increased fALFF and ReHo during active and sham tDCS in sensory and motor regions. A. Significant main effects of tDCS condition (“Main Cond.”) were apparent in regional FC metrics fALFF and ReHo in nodes overlapping sensory and motor cortex ($p(\text{fdr}) < 0.05$). B. In pairwise contrasts of tDCS conditions (active/sham/rest) in these nodes, regional fALFF and ReHo during both active and sham tDCS was greater than for the rest condition in most nodes ($p < 0.05$). From left to right, the cortical surface views in A and B are: left and right lateral, superior temporal plane insets (left on top), left and right medial, and dorsal (left on bottom) surfaces. No significant effects were apparent for contrasts not shown (i.e., Rest > Active, Rest > Sham, Active > Sham). C. Mean fALFF is plotted for representative nodes marked with asterisks in A, including primary visual, auditory, and somatosensory cortex (PVC, PAC, PSC, respectively), as well as posterior cingulate cortex

(PCC). Black whiskered error bars reflect standard error of the mean, and thick gray reflect 95% confidence intervals (within subjects). Individual datapoints are also plotted in color to reflect tDCS montage (red DLPFC, green LTA, blue STC). Double asterisks on plots mark $p(\text{fdr}) < 0.05$ from the main analysis; single asterisks mark pairwise contrasts $p < 0.05$; daggers mark pairwise contrasts $p < 0.10$.

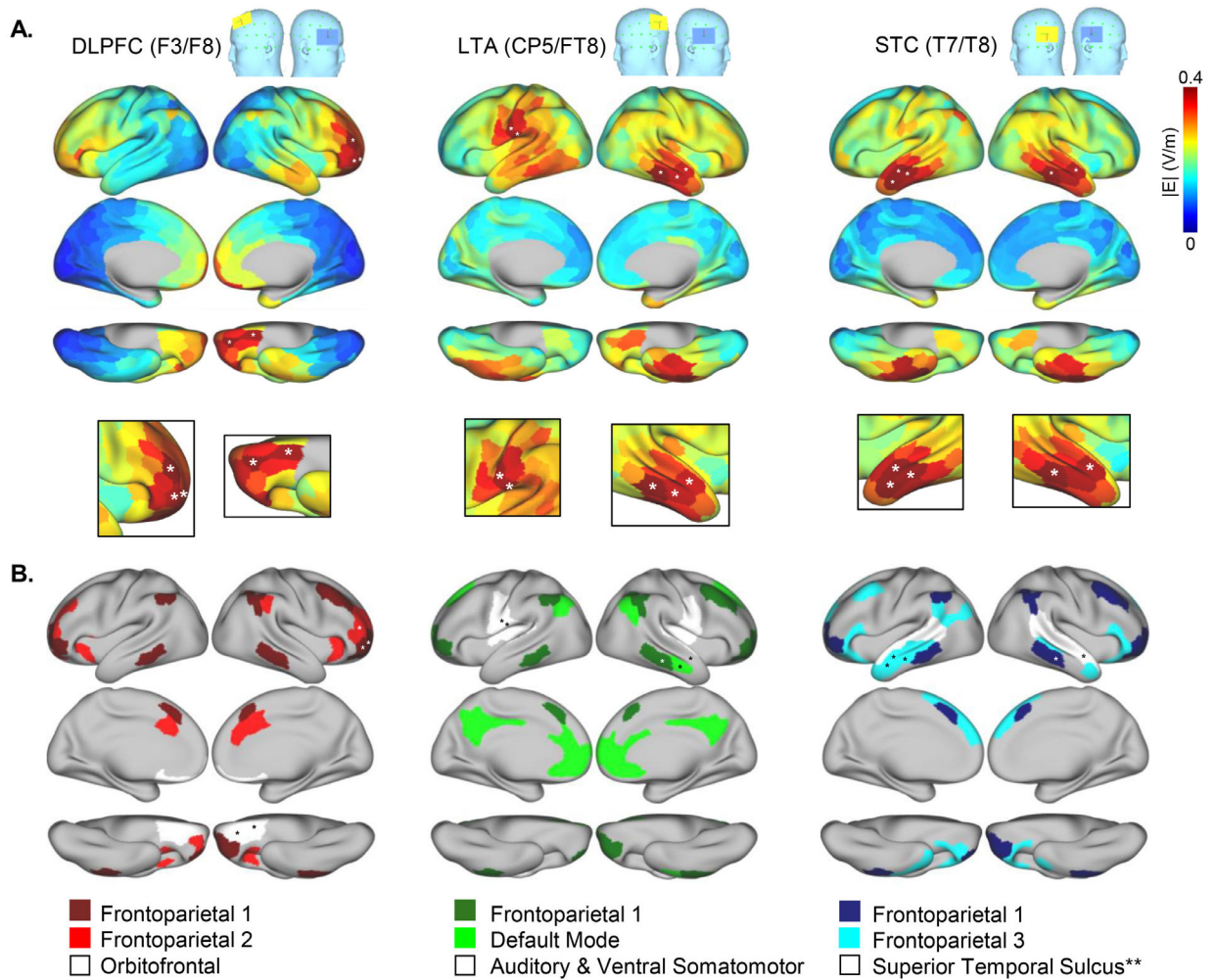


Fig. 3.

High E field nodes and networks. A. E field magnitude is plotted for each node on template cortical surfaces for each electrode montage. White asterisks mark the locations of the five nodes with greatest E field magnitude (i.e., $|E|$ in V/m) for each montage, estimated using a single template head. B. Resting state networks (RSNs) that contain one or more of the top five nodes identified in A are displayed for each montage. **Note that the “Superior Temporal Sulcus” network was also a high E field network for the LTA (CP5/TP8) montage. Numbers given in the color keys at bottom match the RSN numbers displayed in Fig. 1B and Yeo et al. 2011 indices. In A and B, cortical surfaces are lateral, medial, and ventral displayed from top to bottom.

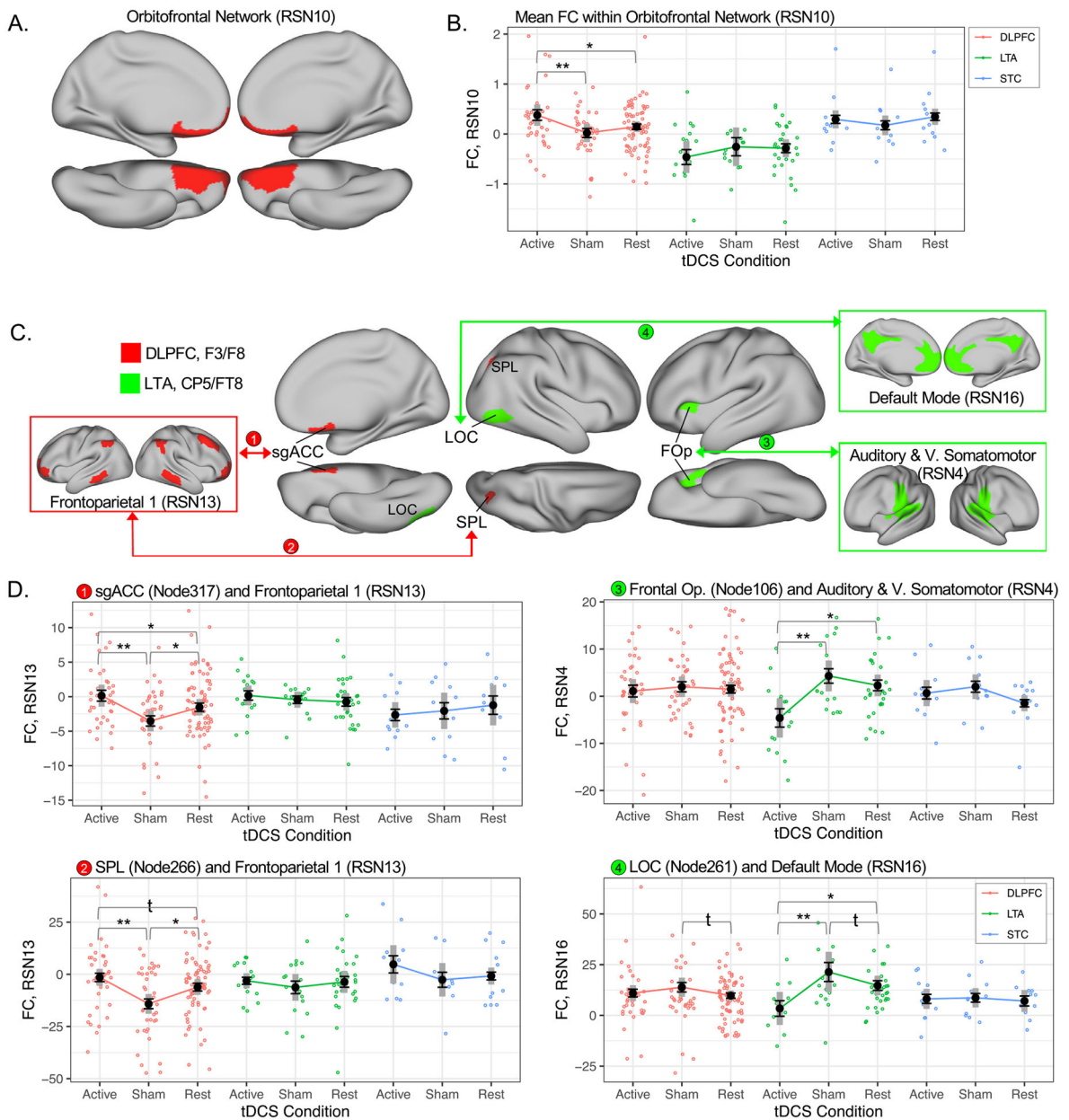


Fig. 4. Active tDCS influences connectivity in high E field networks. A. Mean functional connectivity (Global FC) increased within a high E field network during active DLPFC-tDCS compared with sham. Cortical surface views are left and right medial (top row) and left and right ventral (bottom row). B. Mean global FC for the Orbitofrontal Network is plotted for each montage and condition; black whiskered error bars reflect standard error of the mean, and thick gray bars reflect 95% confidence intervals (within subjects). Individual datapoints are plotted in color to reflect tDCS montage (red DLPFC, green LTA, blue STC). Double asterisks on plots mark $p(\text{fdr}) < 0.05$ from the main analysis; single asterisks mark pairwise contrasts $p < 0.05$; daggers mark pairwise contrasts $p < 0.10$. C. FC decreased between specific nodes and networks with high E field magnitude during active DLPFC-

tDCS (red) and active LTA-tDCS (green). High E field networks are displayed in boxes, nodes are displayed in patches on cortical surfaces, and arrowed lines connect node-network pairs exhibiting significant differences in FC between active and sham conditions for a given montage of interest. D. FC is plotted for each node-network connection in C (numbered 1–4) using the same conventions as in B. RSN and Node numbers reflect indices from Yeo et al. 2011 and Schaeffer et al. 2017, respectively. RSN FC metrics plotted in B and D are beta (parameter) estimates from FSL dual regression.

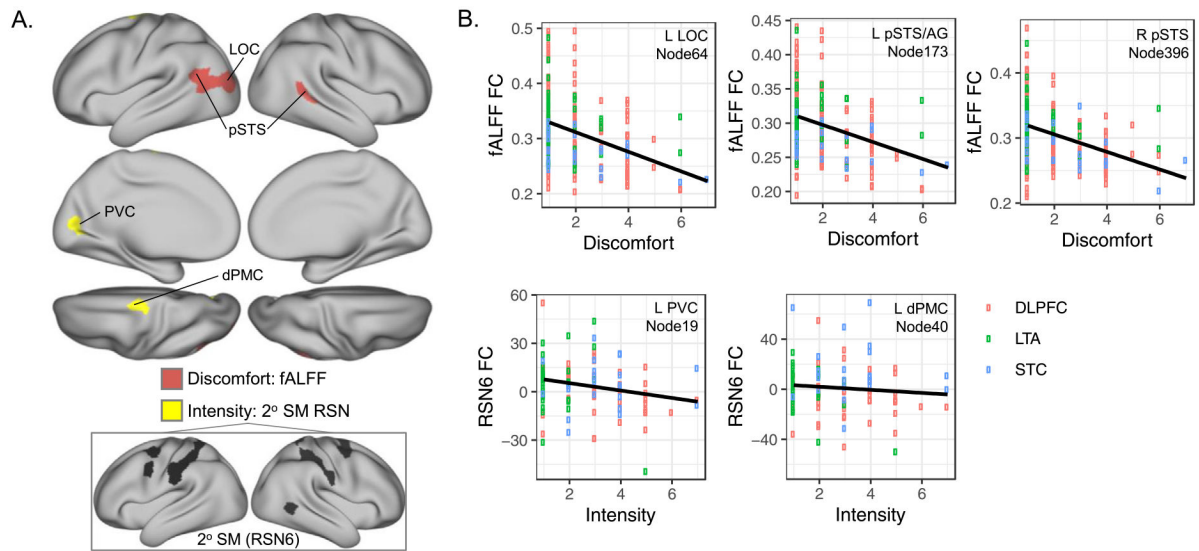


Fig. 5. Ratings of tDCS discomfort and intensity associate with functional connectivity (FC) metrics during active and sham conditions. A. Patches on cortical surfaces mark nodes where FC metrics showed linear relationships with participant ratings of tDCS-related discomfort (salmon) and intensity (yellow), respectively (10-pt scale). B. FC (y axis) is plotted for tDCS-related discomfort and intensity (x axes) for the nodes identified in A. Open circles reflect data for active and sham conditions in each participant with color indicating montage. Linear regression and fit lines are plotted in black and gray, respectively. RSN and Node numbers reflect indices from Yeo et al. 2011 and Schaeffer et al. 2017, respectively. RSN6 FC metrics plotted in B are beta (parameter) estimates from FSL dual regression.

Table 1

Participant characteristics and tDCS ratings.

	DLPFC	LTA	STC
n	37	16	11
Age, mean(SE) ^a	32.03(1.95)	34.00(3.80)	38.91(2.90)
Sex, female(male) ^b	22(15)	10(6)	2(9)
Handedness, Right(Left)Both ^c	34(2)1	12(3)1	10(1)0
Intensity, Active tDCS, mean(SE) ^d	3.15(0.28)	1.69(0.28)	3.91(0.51)
Intensity, Sham tDCS, mean(SE) ^d	3.00(0.31)	1.81(0.44)	3.91(0.51)
Discomfort, Active tDCS, mean(SE) ^e	2.28(0.22)	1.25(0.14)	2.81(0.66)
Discomfort, Sham tDCS, mean(SE) ^e	2.00(0.22)	1.56(0.33)	1.82(0.26)
Site, UCLA(NU)	19(18)	16(0)	1(10)

Abbreviations: dorsolateral prefrontal cortex, DLPFC; lateral temporoparietal area, LTA; superior temporal cortex, STC; transcranial direct current stimulation, tDCS; major depressive disorder, MDD.

^aNo difference in age between 3 montage groups $F(2,61)=1.3$ $p=0.28$.

^bProportion of male volunteers was greater for the STC group $\chi^2(2)=8.5$ $p=0.01$.

^cNo difference in handedness across 3 montage groups $\chi^2(4)=3.4$ $p=0.50$.

^dIntensity ratings lower for LTA montage $F(2102)=10.3$ $p<0.001$.

^eDiscomfort ratings lower for LTA montage $F(1114)=7.4$ $p=0.01$.